Electronic Supporting Information

Crystals Springing Into Action: Metal-Organic Framework CUK-1 as a Pressure-Driven Molecular Spring

Paul Iacomi,[a] Ji Sun Lee,[b] Louis Vanduyfhuys,[c] Kyung Ho Cho,[b] Pierre Fertey,[d] Jelle Wieme,[c]

Dominique Granier,[a] Guillaume Maurin,[a] Veronique Van Speybroeck,[c] Jong-San Chang [b]

and Pascal G. Yot*[a]

a. ICGM, University Montpellier, CNRS, ENSCM, F-34095 Montpellier, France. e-mail: pascal.yot@umontpellier.fr; Tel.: +33 4 67 14 32 94; Fax: +33 4 67 14 42 90.

b. Research Center for Nanocatalysts, Korea Research Institute of Chemical Technology, Yusung, Daejeon 305-600, Korea.

c. Centre for Molecular Modeling, Ghent University, Technologiepark 903, B-9052 Zwijnaarde, Belgium. Centre for Molecular Modeling, Ghent University, Technologie park 903, B-9052 Zwijnaarde, Belgium.

d. Synchrotron Soleil, L'orme des Merisiers, Saint-Aubin - BP 48, F-91192 Gif-sur-Yvette cedex, France.

1.   Synthesis methodology

1.1.   Synthesis of CUK-1(Co) single crystal

An aqueous solution of ligand precursor was prepared by mixing the 2,4-pyridinedicarboxylic acid (0.74 g, 4.43 mmol) to aqueous KOH solution (1.0 M, 18.0 cm^3), which was subsequently added to a stirred aqueous solution (18.0 cm^3) of $CoCl_2 \bullet 6H_2O$ (1.428 g, 6.0mmol) to obtain a gel-like reaction mixture. The resulting viscous mixture was heated to 473 K in a 100 cm^3 Teflon-lined autoclave reactor over 48 h, and then cooled to room temperature over 6 h. The crystalline solid was purified by short cycles (3×20 s) of ultrasonic treatment in H_2O (100 cm^3), followed by decanting of the cloudy supernatant. Pure pink prismatic large crystals of CUK-1(Co) were obtained after drying at 373 K for 12 h.

1.2. Synthesis of CUK-1(Co) powder sample

An aqueous solution of ligand precursor was prepared by mixing the 2,4-pyridinedicarboxylic acid (1.11 g, 6.64 mmol) to aqueous KOHsolution (1.0 M, 18.0 cm³), which was subsequently added to a stirred aqueous solution (18.0 cm³) of $CoCl_2\bullet 6H_2O$ (2.142 g, 9.0 mmol) to obtain a gel-like reaction mixture. The resulting viscous mixture was heated to 473 K in a 100 cm³ Teflon-lined autoclave reactor over 15 h, and then cooled to room temperature over 6 h. The crystalline solid was purified by short cycles (3×20 s) of ultrasonic treatment in H_2O (100 cm³), followed by decanting of the cloudy supernatant. Pure pink prismatic particles of CUK-1(Co) were obtained after drying at 373 K for 12 h.

1.3. Synthesis of CUK-1(Mg) powder sample

A aqueous solution of ligand precursor was prepared by mixing the 2,4-pyridinedicarboxylic acid (1.59 mg, 8.57 mmol) to aqueous KOH solution (1.0 M, 27.4 cm³), which was subsequently added to a stirred solution (29.0 cm³) of $Mg(NO_3)_2\bullet 6\ H_2O$ (3.08 g, 12.0 mmol) to obtain a gel-like slurry, which was then transferred to a 100 cm³ teflon-lined autoclave reactor, heated at 483 K for 15 h, and cooled for 6 h. After cooling, the crystalline solid was purified by brief cycles of sonication in fresh H_2O (100 cm³), followed by decantation of the cloudy supernatant to yield large, colourless prismatic particles of CUK-1(Mg) after drying at 373 K for 12 h.

2. Sample characterization

2.1. Surface area

The Brunauer-Emmett-Teller (BET) area is typically obtained from N2 adsorption performed at 77 K, however since the amount of adsorbed N_2 in CUK-1 materials is very limited at 77 K, CO_2 adsorption isotherms at 196 K measured in a Tristar 3020 were used as an alternative to calculate the BET areas of the samples. Prior to CO_2 adsorption, the samples were activated at 573 K for 12 h under vacuum. The BET area was calculated from CO_2 isotherm points within the range of 0.005-0.3 P/P°, assuming a CO_2cross-sectional area of 17.0 Å² per molecule and the pore volume was obtained by a single point method at P/P°=0.99.
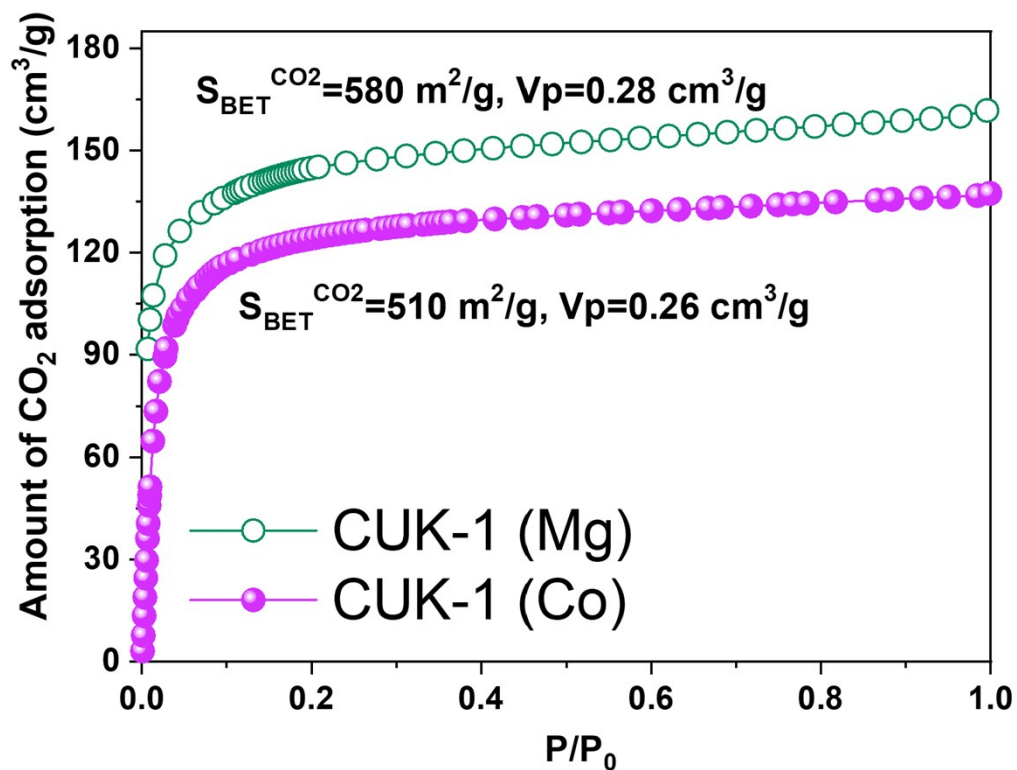
Figure S1: *CO_2 adsorption isotherm of CUK-1 (Mg and Co) measured at 196 K after activation at 573 K for 12 h under vacuum.*

2.2. Thermogravimetry

Thermogravimetric (TG) analysis was performed in a thermogravimetric analyzer (DT Q600, TA Instruments, Universal V4.5A) under dry N_2 flow of 100 ml.min^{-1} with a heating rate of 5 K.min^{-1}. Before each TGA measurement, samples were hydrated in a chamber with 70% RH at 30°C for 1 day.
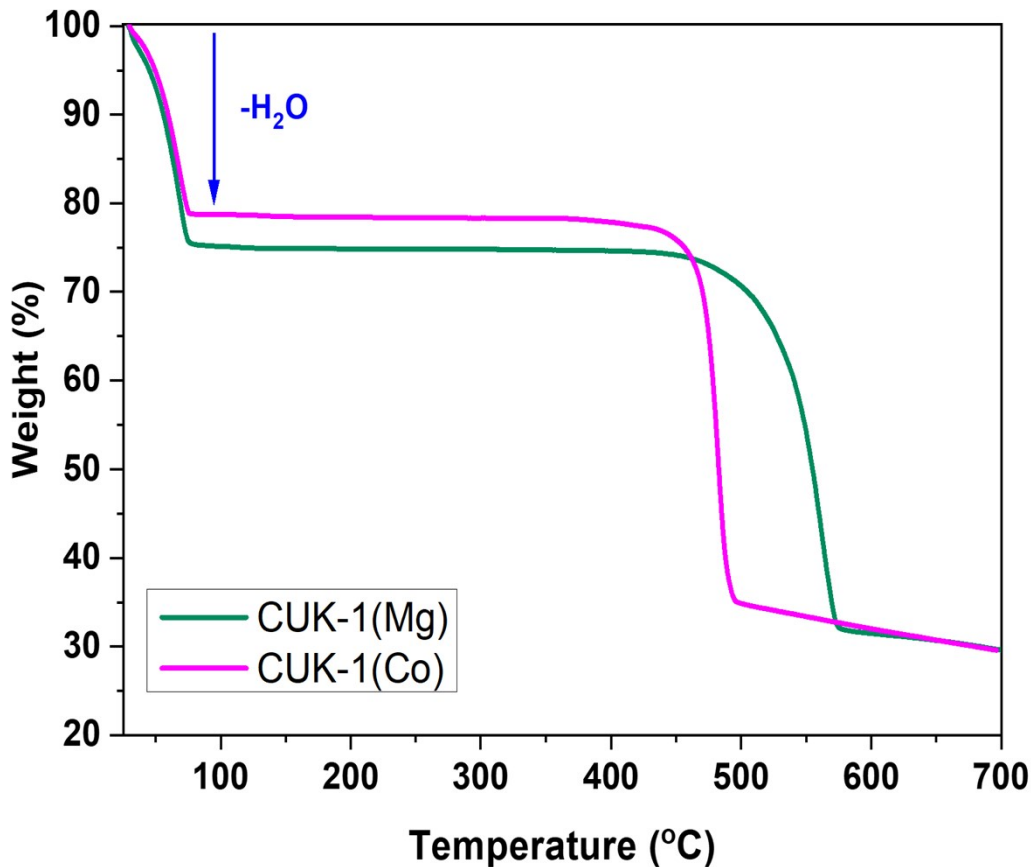
Figure S2: *TG profiles of hydrated CUK-1 (Mg and Co) measured under N₂ flow.*

3. Powder X-ray diffraction

3.1. Methodology

Powder samples were activated at 250°C under secondary vacuum (1e-3 mbar) overnight (for 8 h), then transferred in a 1 mm diameter quartz capillary in an argon glovebox. After flame sealing, the capillaries were used to collect diffraction patterns with a a Bruker D8 Discover and a Panalytical X'Pert XRPD diffractometers for Co- and Mg- based CUK-1 respectively, in a Debye-Scherrer geometry using monochromated Cu-K$_{\alpha 1}$ radiation.

The Rietveld refinement of the pattern in the angular domain 5°–100° in 2θ was carried out using a Pseudo-Voigt peak shape with a cut-off of 12. A manual background combined with a 36 term Chebyshev polynomial function was used in the refinement. The positions of the N, O and C atoms were refined using the rigid body procedure available in the JANA2006 suite [1] by considering the

phenyl rings and carboxylate groups as plane and rigid, and the isotropic thermal parameters (U_{iso}) were constrained to be identical for all atom types.

3.2. Refined structures

The CIF files of resulting structures are attached as Electronic Supplementary Information.

Table S1: *Formulae, unit cell parameters and volume of the two pristine op forms of CUK-1(M) samples characterised in this work, as obtained from Rietveld refinement of PXRD data and compared to previously-published data.*

CUK-1(M)	Co		Mg	
Formulae	$C_{14}H_6Co_3N_2O_{10}$		$C_{14}H_6Mg_3N_2O_{10}$	
Molar Mass (g/mol)	541.01		435.12	
Laue class	2/m		2/m	
Crystal system	monoclinic		monoclinic	
Space Group	*C2/c* (No. 15)		*C2/c* (No. 15)	
Z	4		4	
R_p	9.66		10.25	
wR_p	16.68		13.35	
GoF	3.23		2.17	
U.C. parameters	This work	Humphrey *et al.*[2]	This work	Saccoccia *et al.* [3]
a (Å)	18.1044(6)	18.1020(7)	18.2173(7)	18.180(10)
b (Å)	12.7761(4)	12.7694(5)	12.4949(5)	12.464(8)
c (Å)	10.9645(3)	10.9701(5)	11.0412(4)	11.005(6)
β (°)	103.361(3)	103.4004(16)	102.710(3)	102.778(16)
U.C. Volume (Å^3)	2466.72(18)	2467.48(14)	2451.64(16)	2432(2)
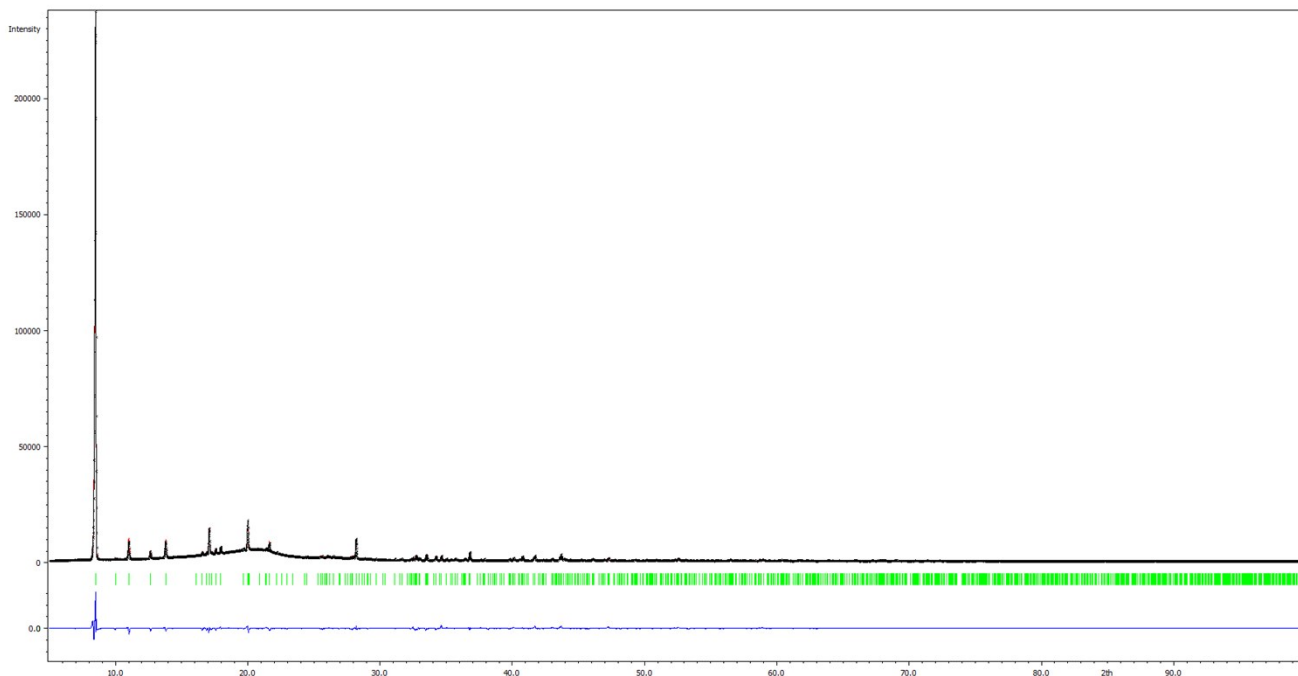
Figure S3: *Rietveld refinement of the unit cell of the diffraction pattern obtained for CUK-1(Co) powder in its pristine open form (GoF = 3.23, Rp = 9.66, wRp = 16.68).*

Table S2: *Rietveld-refined atomic positions of the open CUK-1(Co) powder asymmetric unit.*

Label	Element	x	y	z	U_{iso}	Pos	Occupancy
Co1	Co	0.0809(4)	0.0279(4)	0.0371(6)	0.0667(15)	8f	1
Co2	Co	0	0.0924(6)	0.25	0.0667(15)	4d	1
N1	N	0.172261	-0.070219	0.112687	0.0667(15)	8f	1
O1	O	0.0625(10)	-0.0397(14)	0.2210(14)	0.0667(15)	8f	1
O2	O	0.1279(8)	-0.0848(14)	0.4101(19)	0.0667(15)	8f	1
O3	O	0.3451(10)	-0.3476(15)	0.3668(15)	0.0667(15)	8f	1
O4	O	0.3886(10)	-0.3044(14)	0.1979(14)	0.0667(15)	8f	1
O5	O	-0.0229(13)	0.0964(15)	0.0623(17)	0.0667(15)	8f	1
C2	C	0.181095	-0.103765	0.231545	0.0667(15)	8f	1
C3	C	0.237692	-0.17073	0.288241	0.0667(15)	8f	1
C4	C	0.290106	-0.206039	0.222924	0.0667(15)	8f	1
C5	C	0.282898	-0.16753	0.103199	0.0667(15)	8f	1
C6	C	0.2232(13)	-0.101(2)	0.0475(12)	0.0667(15)	8f	1
C7	C	0.1194(6)	-0.0744(7)	0.2953(19)	0.0667(15)	8f	1
C8	C	0.3452(5)	-0.2946(8)	0.2710(13)	0.0667(15)	8f	1
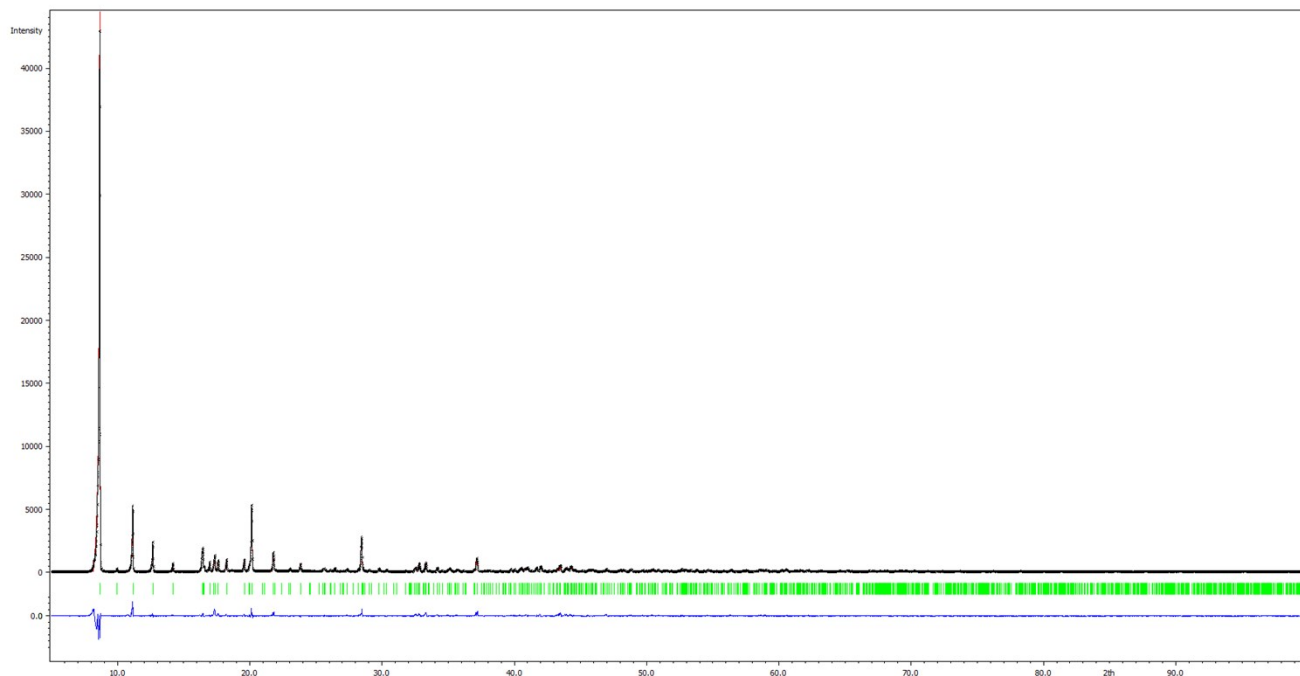
Figure S4: *Rietveld refinement of the unit cell of the diffraction pattern obtained for CUK-1(Mg) powder in its pristine open form (GoF = 2.17, Rp = 10.25, wRp = 13.35).*

Table S3: *Rietveld-refined atomic positions of the open CUK-1(Mg) powder asymmetric unit.*

Label	Element	x	y	z	U_{iso}	Pos	Occupancy
Mg1	Mg	0.0838(4)	0.0383(6)	0.0412(8)	0.0064(6)	8f	1
Mg2	Mg	0	0.1045(9)	0.25	0.0064(6)	4d	1
N1	N	0.185474	-0.069741	0.099063	0.0064(6)	8f	1
O1	O	0.0778(5)	-0.0156(8)	0.2157(8)	0.0064(6)	8f	1
O2	O	0.1367(6)	-0.0914(9)	0.3924(9)	0.0064(6)	8f	1
O3	O	0.3559(6)	-0.3296(9)	0.3650(9)	0.0064(6)	8f	1
O4	O	0.4220(6)	-0.2774(9)	0.2284(10)	0.0064(6)	8f	1
O5	O	-0.0219(7)	0.0922(10)	0.0484(11)	0.0064(6)	8f	1
C2	C	0.189178	-0.107903	0.214667	0.0064(6)	8f	1
C3	C	0.246569	-0.171334	0.276231	0.0064(6)	8f	1
C4	C	0.305249	-0.19785	0.219809	0.0064(6)	8f	1
C5	C	0.303013	-0.154526	0.103838	0.0064(6)	8f	1
C6	C	0.247761	-0.080961	0.05352	0.0064(6)	8f	1
C7	C	0.1295(3)	-0.0688(5)	0.2807(9)	0.0064(6)	8f	1
C8	C	0.3666(3)	-0.2750(5)	0.2765(7)	0.0064(6)	8f	1

7

4. Porosimetry

4.1. Methodology

The hydrostatic compression experiments were performed using a Hg porosimeter (Micromeritics Autopore 9240) on previously activated powdered MOF samples. The pressure applied can vary in the range of 0.1 MPa–413 MPa. About 0.2 g of materials was placed in a sample cell then outgassed in-situ at 6.5 Pa for 1 h, then filled with mercury and compressed in an oil bath. The Hg intruded volume is corrected for the intrinsic compressibility of mercury and any expansion of the unit by a blank measurement using the same sample tube. The steps present in the mercury intrusion curve below 10 MPa correspond to the filling of the penetrometer, the interparticle porosity and textural effects.

In the explored range of pressure, Washburn's law states that the relationship between the applied pressure and filled cylindrical pores is:

$$P = -\frac{4\gamma\cos\theta}{d}$$

with γ as mercury surface tension and θ the surface contact angle of 0.485 N/m and 130° respectively. According to the aforementioned equation pore diameters accessible for Hg would range in the interval 35–400 Å. Considering the pore size of CUK-1 frameworks ($\approx$ 9 Å) and pressure range explored by mercury intrusion ($P_{max} = $ 420 MPa), the non-wetting mercury cannot penetrate into the pores, hence the pressure increase induces an isostatic pressure on the crystallites. The Hg intruded volume mercury is then directly related to the volumetric strain corresponding to the compressibility of the material.

4.2. CUK-1(Co) Hg intrusion curve

Complete (4 cycle) intrusion-extrusion corresponding to CUK-1(Co) powder. Raw data available as Electronic Supplementary Information.
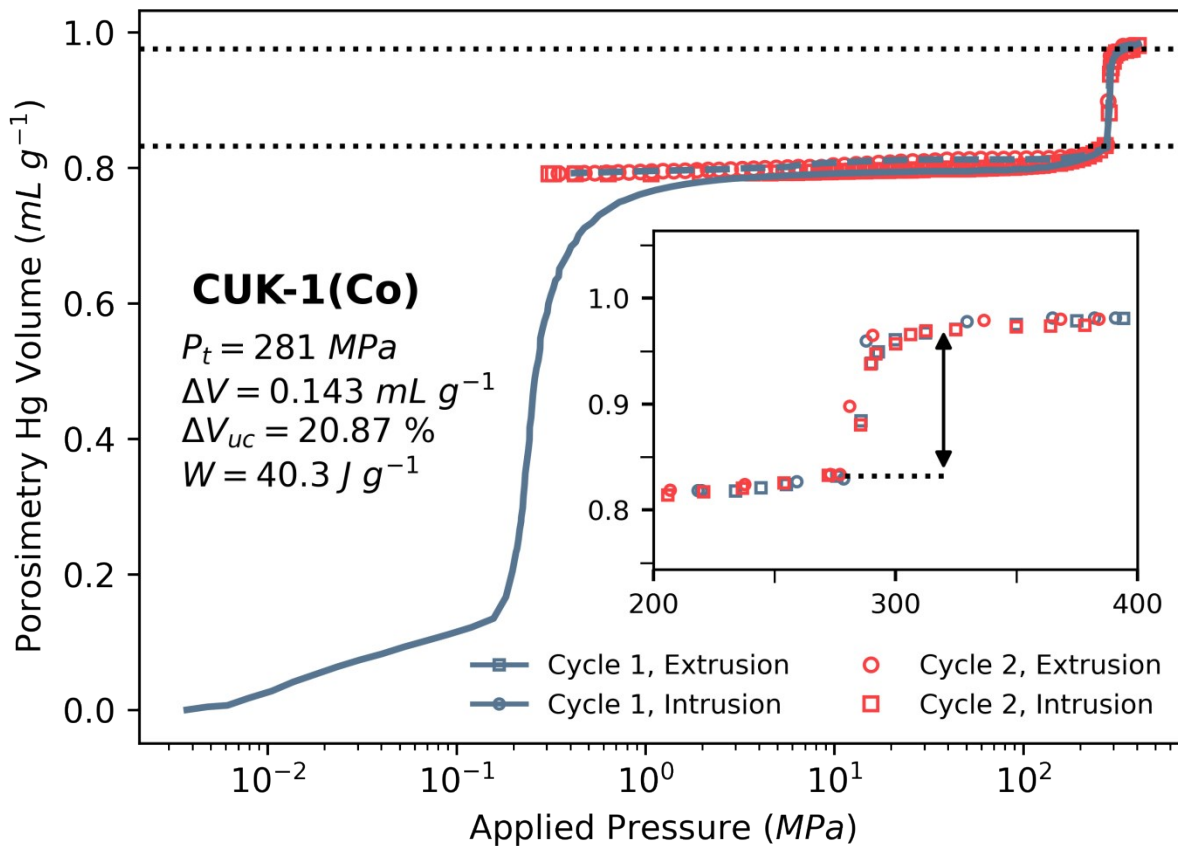
Figure S5: *Four sequential mercury intrusion-extrusion curves on CUK-1(Co) powder. Line is a guide for the eye. Volume below 1 MPa corresponds to powder compaction and intercrystallite void filling. Dotted horizontal lines demarcate contraction lower and upper bounds. Inset highlights the intrusion step in a linear scale with the op/cp contraction marked with an arrow.*

4.3. CUK-1(Mg) Hg intrusion curve

Intrusion-extrusion corresponding to CUK-1(Mg) powder. Raw data available as Electronic Supplementary Information.
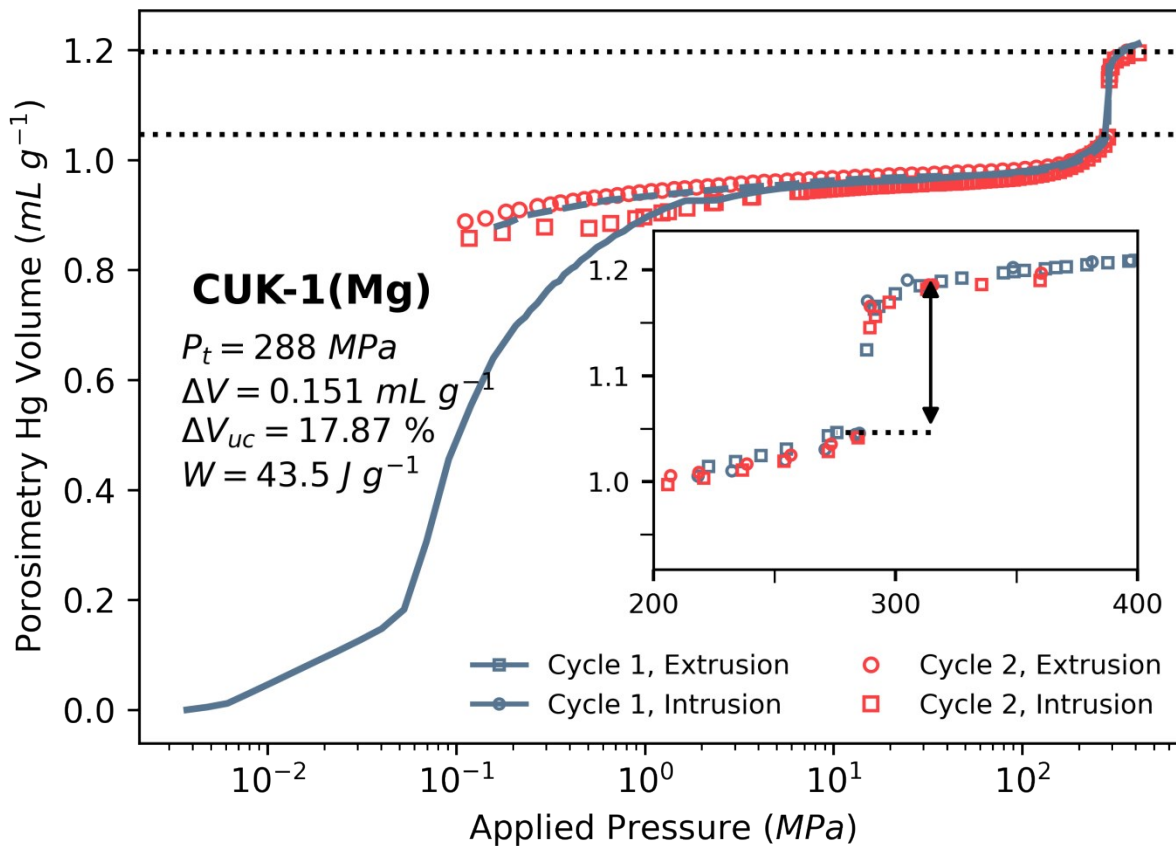
Figure S6: *Two sequential mercury intrusion-extrusion curves recorded on CUK-1(Mg) powder, denoted as a line and as empty symbols, respectively. Initial Hg intruded volume corresponds to powder compaction and intercrystallite void filling. Dotted horizontal lines demarcate the MOF contraction lower and upper bounds, while the inset highlights the intrusion step using a linear pressure scale with the op/cp contraction marked with an arrow.*

5. Energy density of CUK-1

Besides specific gravimetric energy W_g it is useful to also consider energy density (energy per unit volume, W_v) of CUK-1 when compared to other systems, in particular in the case of water intrusion in hydrophobic zeolites. As seen in Table S4, CUK-1(Co) shows a relatively high density that makes its volumetric energy storage capacity attractive, when compared with the corresponding densities of the best performing water-intrusion zeolites from Fraux et al. [4]

Table S4: *Density, gravimetric energy density and volumetric energy density for CUK-1(Co) and in zeolite + water intrusion systems. Density of CUK-1(Co) is determined as ideal crystal density.*

Material	ρ (cm^3.g^{-1})	W_g (J.g^{-1})	W_v (J.cm^{-3})
CUK-1(Co)	1.46	40	58.4
Silicalite-1 (MFI net)	1.97	10.6	20.8
ZSM-12 (MTW net)	1.93	15	28.9
Ferrierite (FER net)	2.13	15	31.9

6. High pressure single crystal X-ray diffraction

6.1 Methodology

To apply hydrostatic pressure *in operando*, a gas operated membrane diamond anvil cell was used, with a 40° opening and 500 µm polished diamond culets. A pre-indented and pre-drilled steel gasket is used to ensure an enclosed environment. The sample was activated at 250°C before being transferred into the gasket in a nitrogen-filled glovebox. A drop of silicone oil AP-100 (from Sigma-Aldrich) was used as a non-intruding hydrostatic pressure transmitting medium. A small gold flake was also introduced into the gasket to act as a pressure standard. Data collection was carried out at the CRISTAL beamline of the SOLEIL synchrotron using a monochromatic wavelength λ=0.5137 Å (24 keV) beam collimated to 50x50 µm, and recorded on a 2D RayoniX SX-165 CCD detector.

Data integration was performed in CrysAlysPro, up to a resolution of 0.92 Å, a rejection angle calculated from the 40° opening of the DAC. The ABSPACK routines were used to scale integrated intensities through an empirical adsorption correction. Structural solution was carried out with a dual space recycling algorithm in an expanded *P1* setting by SHELXT [5], using OLEX2 [6] as a frontend. Further refinements based on F² were performed using SHELXL. [7] Hydrogen atoms were refined using a riding model, with the μ_3-O hydrogen constrained as tetrahedral. Additional planar restraints were imposed on the atoms of the pyridine ring. Since inert nitrogen from the glovebox is still present in the

material pores, residual electron density in the porous voids was masked with a solvent mask, as implemented in the BYPASS/SQUEEZE routine in OLEX. As pressure was applied, crystal cracking could be observed as a secondary set of reflections. If the sets were sufficiently separated, individual crystallites were treated as twins and unit cell refinement was performed independently. Due to minimal reflection overlap and the lower intensity of the second crystallite, after scaling and deconvolution only the first set was used for structure solution and refinement. Upon higher pressure application (above 1 GPa), extensive crystal cracking prevented meaningful structure solution.

To ascertain the pressure inside the gasket, separate acquisitions of the Au foil were taken. Resulting 2D images were subsequently azimuthally integrated using Dioptas [8] as a graphical interface to pyFAI. [9] Unit cell parameters were then cyclically refined in JANA2006 [1] through structure-independent refinement in a cubic system, starting from the ambient pressure cell dimensions. The as-determined a unit cell parameter was used to calculate pressure using the equation of state provided by Dubrovinsky *et al*. [10]

6.2. CUK-1(Co) indexed unit cell dimensions

The unit cell dimensions of the CUK-1(Co) single crystal were indexed using the routines available in CrysAlysPro.

Table S5: *Single crystal indexing for CUK-1(Co) at increasing hydrostatic pressures.*

Pressure (GPa)	0.000	0.309	0.508	0.685	0.933	1.264	1.460	1.751
Laue class	2/m	2/m	2/m	2/m	2/m	2/m	2/m	2/m
Crystal system	monoclinic	monoclinic	monoclinic	monoclinic	monoclinic	monoclinic	monoclinic	monoclinic
Space Group	*C2/c*	*C2/c*	*C2/c*	*C2/c*	*C2/c*	*C2/c*	*C2/c*	*C2/c*
a (Å)	17.988(8)	18.974(3)	19.6026(9)	19.6011(9)	19.6231(11)	19.6331(11)	19.761(5)	19.867(12)
b (Å)	13.0762(11)	11.0427(15)	9.2014(9)	9.2018(9)	8.8091(11)	8.7778(11)	8.513(3)	8.576(13)
c (Å)	10.864(7)	10.9677(6)	11.0368(3)	11.0360(4)	11.0233(4)	11.0230(4)	11.0172(14)	11.063(5)
β (°)	103.82(7)	100.796(9)	99.434(3)	99.435(3)	99.356(4)	99.342(4)	99.5(13)	99.82(5)
U.C. Volume (Å^3)	2482(2)	2257.4(5)	1963.8(2)	1963.6(2)	1880.2(3)	1874.5(3)	1837.1(9)	1857(3)
R_{int} (%)	19.7	3.11	3.08	3.56	17.6	3.58	12.24	16.5

6.3. CUK-1(Co) cp structure

CIF files of adequately resolved CUK-1(Co) structures under hydrostatic compression (0.309 GPa, 0.508 GPa and 0.685 GPa) have been deposed in CCDC with the identifiers 2019979 to 2019981.

These data can be obtained free of charge from the Cambridge Crystallographic Data Centre. All CIF files can also be found as ESI to this publication.

Table S6: *Single crystal structure data for CUK-1(Co) high pressure structures.*

Pressure (GPa)	0.309	0.508	0.685
Laue class	2/m	2/m	2/m
Crystal system	monoclinic	monoclinic	monoclinic
Space Group	*C2/c*	*C2/c*	*C2/c*
Z	4	4	4
a (Å)	18.974(3)	19.6026(9)	19.6011(9)
b (Å)	11.0427(15)	9.2014(9)	9.2018(9)
c (Å)	10.9677(6)	11.0368(3)	11.0360(4)
β (°)	100.796(9)	99.434(3)	99.435(3)
U.C. Volume (Å^3)	2257.4(5)	1963.8(2)	1963.6(2)
Total reflections	1457	4853	5046
Unique reflections	771	868	916
Completeness	0.5224	0.6596	0.6911
I/σ	34	68.2	52.8
R_{int} (%)	3.11	3.08	3.56
R [Fo > 4sig(Fo)] (%)	5.22	5.53	6.01
wR [all data] (%)	14.90	16.51	17.78
GoF	1.063	1.130	1.158
Largest peak/hole	0.6/-0.5	0.7/-0.7	0.8/-0.8
SQUEEZE'd e$^-$ / U.C.	242	116	130
SQUEEZE V (Å^3)	778	444	436

6.4. CUK-1(Co) op/cp changes

Main differences between the pristine CUK-1(Co) **op** form and the **cp** form (at 0.5 GPa)

Table S7: *Examples of distances, angles and torsions between selected atom pairs, pivots and planes in the open and contracted (at 0.5 GPa) forms of CUK-1(Co). Highlighted in bold are the most important changes, accounting for the differences in conformation between the two structures.*

type	atoms	op	cp@0.5 GPa
distance (Å)	Co1-Co1	3.18	3.17
distance (Å)	Co1-Co2	3.15	3.19
distance (Å)	Co1-O3	2.09	2.11
distance (Å)	Co1-N	2.16	2.16
distance (Å)	Co1-O(OC)	2.06-2.16	2.08-2.09
distance (Å)	Co1-C(OO)	1.48-1.52	1.49-1.54
distance (Å)	O3-O3	2.72	2.79
angle (°)	N-Co1-O5	75.9	75.1
angle (°)	N-Co1-O3	90.9	100
angle (°)	N-Co1-O4	93.6	8f9.8
angle (°)	N-Co1-O6	99	82.4
angle (°)	Co1-O3-Co1	99	96
angle (°)	Co1-O3-Co2	120.9	121
torsion (°)	py-Co2-py	98.3	103.4
torsion (°)	py(CC)-COO	9	2
torsion (°)	py(CE)-COO	20	0.5
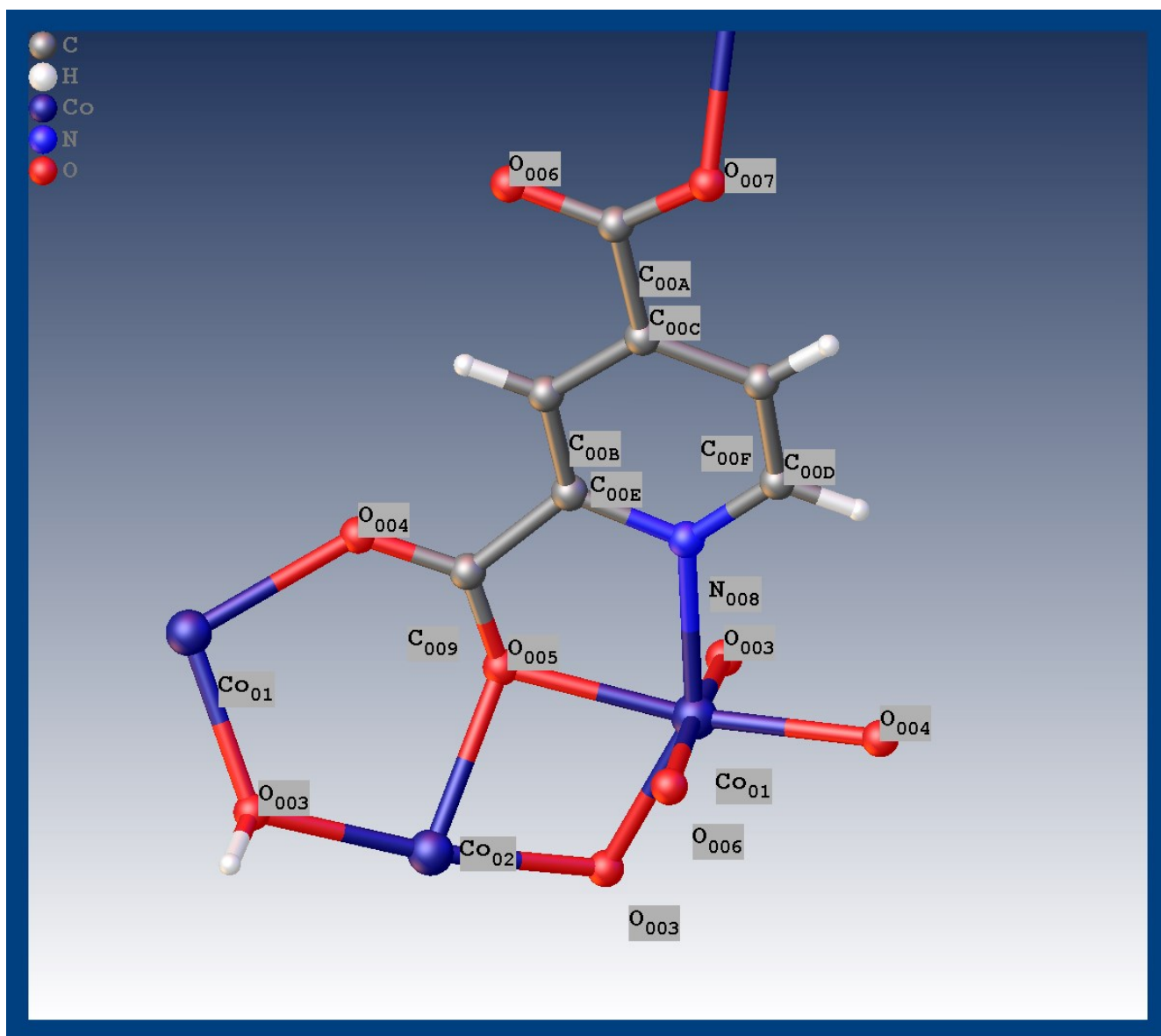
Figure S7: *Diagram of an extended CUK-1 asymmetric unit, labelling the atoms described in 6*

7.   Molecular simulations

7.1   DFT calculations

The DFT calculations for CUK-1(Mg) were performed with the Vienna Ab initio Simulation Package (VASP) [11] with the PBE functional [12,13] including the dispersion correction scheme D3(BJ) introduced by Grimme.[14,15] A plane-wave kinetic energy cutoff of 600 eV and using Gaussian smearing with a smearing width of 0.05 eV were used. A 2×3×4 Monkhorst-Pack k-grid was used. The electronic (ionic) convergence criterion was set to 1e-6 eV (1e-5 eV).

7.2.   *Force field calculations*

A force field was derived for CUK-1(Mg) with QuickFF using the equilibrium geometry and Hessian computed at the DFT level as input. The MCAH configuration of QuickFF was used as outlined in reference No. 15. [16] The electrostatic interactions were described by Coulomb interaction between Gaussian charges derived from the DFT equilibrium wave function using the Minimal Basis Iterative Stockholder [17] analysis scheme as implemented in HORTON. [18] Van der Waals interactions were described using the MM3 force field. [19] Using this newly derived force field, the free energy was computed as function of the unit cell volume from molecular dynamics simulations in the (N, V, σ_a=0, T) ensemble using a protocol outlined in earlier work. [20,21] The resulting pressure and free energy profiles are shown in Fig. S8.

The computed free energy profile clearly shows a single minimum, indicating that the material exhibits a single equilibrium at zero pressure, and corresponds to a lack of hysteresis in the corresponding pressure profile. This is in agreement with the reversible transition without hysteresis that has been observed experimentally. While the computed pressure profile does not exhibit a discontinuous transition, it does show a region around 0 MPa–250 MPa in which the pressure curve flattens, indicating a softening of the material. The experimentally observed transition pressure for CUK-1(Mg) of 233 MPa is well within the pressure range of this softening. Furthermore, we also decomposed the free energy (F=E-T.S) into its internal energy (E) and entropic (-T.S) contributions (see **13**b). As can be derived from this figure, the entropic contributions stabilize the **op** form while destabilize the **cp** form. Hence, it further aids in avoiding the formation of a metastable **cp** form (i.e. avoid local minimum in the F(V) profile at volumes corresponding to the contracted state) leading to a free energy profile that corresponds to an ideal spring-like material with a hysteresis-free reversible transition.
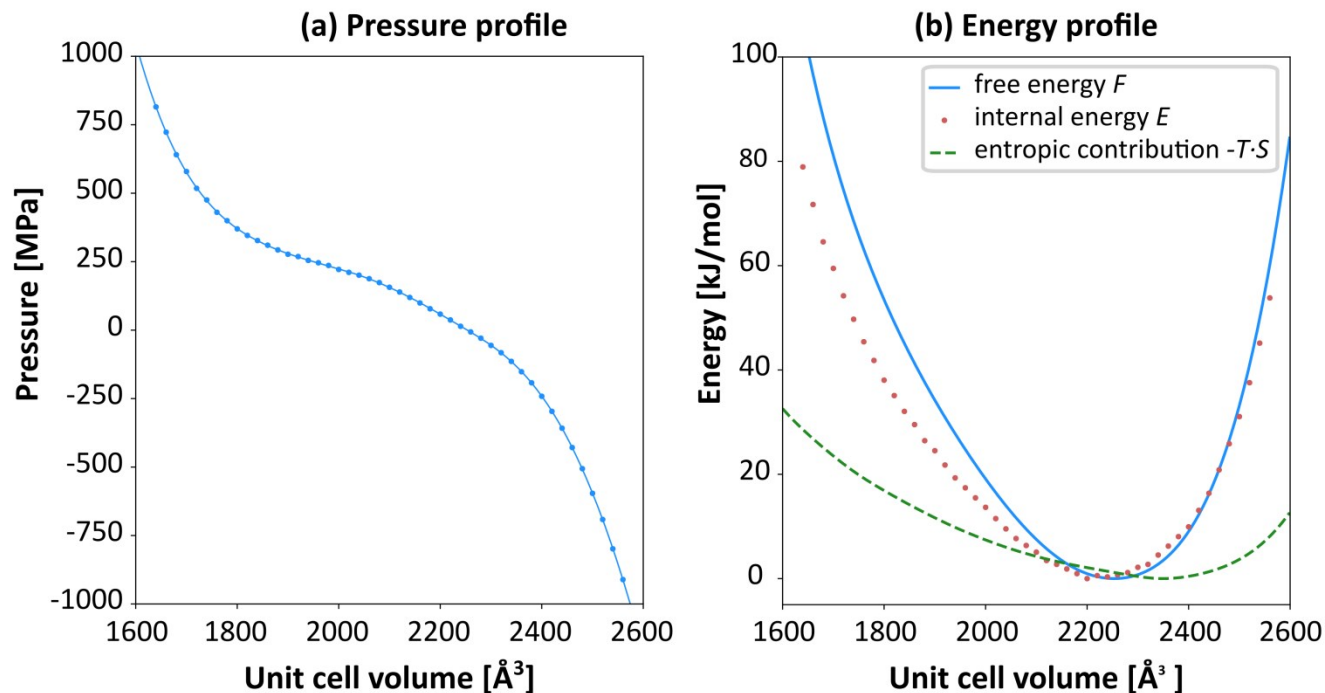
Figure S8: *Pressure (left) and free energy profile (right) of CUK-1(Mg) as function of unit cell volume constructed from molecular dynamics simulations at 300 K.*

REFERENCES

1   V. Petříček, M. Dušek and L. Palatinus, Zeitschrift für Kristallographie - Crystalline Materials, , DOI:10.1515/zkri-2014-1737.

2   S. M. Humphrey, J.-S. Chang, S. H. Jhung, J. W. Yoon and P. T. Wood, Angew. Chem. Int. Ed., 2007, 46, 272–275.

3   B. Saccoccia, A. M. Bohnsack, N. W. Waggoner, K. H. Cho, J. S. Lee, D.-Y. Hong, V. M. Lynch, J.-S. Chang and S. M. Humphrey, Angew. Chem. Int. Ed., 2015, 54, 5394–5398.

4   G. Fraux, F.-X. Coudert, A. Boutin and A. H. Fuchs, Chemical Society Reviews, 2017, 46, 7421–7437.

5   G. M. Sheldrick, Acta Crystallogr A Found Adv, 2015, 71, 3–8.

6   O. V. Dolomanov, L. J. Bourhis, R. J. Gildea, J. A. K. Howard and H. Puschmann, J Appl Crystallogr, 2009, 42, 339–341.

7   G. M. Sheldrick, Acta Crystallogr C Struct Chem, 2015, 71, 3–8.

8   C. Prescher and V. B. Prakapenka, High Pressure Research, 2015, 35, 223–230.

9   J. Kieffer and D. Karkoulis, J. Phys.: Conf. Ser., 2013, 425, 202012.

10   L. Dubrovinsky, N. Dubrovinskaia, E. Bykova, M. Bykov, V. Prakapenka, C. Prescher, K. Glazyrin, H.-P. Liermann, M. Hanfland, M. Ekholm, Q. Feng, L. V. Pourovskii, M. I. Katsnelson, J. M. Wills and I. A. Abrikosov, Nature, 2015, 525, 226–229.

11   G. Kresse and J. Furthmüller, Phys. Rev. B, 1996, 54, 11169–11186.

12   J. P. Perdew, K. Burke and M. Ernzerhof, Physical Review Letters, 1996, 77, 3865–3868.

13   J. P. Perdew, K. Burke and M. Ernzerhof, Phys. Rev. Lett., 1997, 78, 1396–1396.

14   S. Grimme, J. Antony, S. Ehrlich and H. Krieg, The Journal of Chemical Physics, 2010, 132, 154104.

15   S. Grimme, S. Ehrlich and L. Goerigk, J. Comput. Chem., 2011, 32, 1456–1465.

16   L. Vanduyfhuys, S. Vandenbrande, J. Wieme, M. Waroquier, T. Verstraelen and V. Van Speybroeck, J. Comput. Chem., 2018, 39, 999–1011.

17   T. Verstraelen, S. Vandenbrande, F. Heidar-Zadeh, L. Vanduyfhuys, V. Van Speybroeck, M. Waroquier and P. W. Ayers, J. Chem. Theory Comput., 2016, 12, 3894–3912.

18   T. Verstraelen, P. Tecmer, F. Heidar-Zadeh, C. Gonzalez-Espinosa, M. Chan, T. D. Kim, K. Boguslawski, S. Fias, S. Vandenbrande, D. Berrocal and P. W. Ayers, HORTON 2.1.1, 2017.

19   N. L. Allinger, Y. H. Yuh and J. H. Lii, J. Am. Chem. Soc., 1989, 111, 8551–8566.

20   L. Vanduyfhuys, S. M. J. Rogge, J. Wieme, S. Vandenbrande, G. Maurin, M. Waroquier and V. Van Speybroeck, Nature Communications, 2018, 9, 204.

21   S. M. J. Rogge, L. Vanduyfhuys, A. Ghysels, M. Waroquier, T. Verstraelen, G. Maurin and V. Van Speybroeck, J. Chem. Theory Comput., 2015, 11, 5583–5597.